JOURNAL OF Materials CHEMISTRY

Infrared and Raman studies of the κ-phase charge-transfer salts formed by BEDT-TTF and magnetic anions $M(CN)_6^{3-}$ (where $M = Co^{III}$, Fe^{III}, Cr^{III})

Roman Świetlik,*[a] Maria Połomska,[a] Lahcene Ouahab[b] and Joseph Guillevic[b]

[a]*Institute of Molecular Physics, Polish Academy of Sciences, Mariana Smoluchowskiego 17, 60-179 Poznań, Poland. E-mail: swietlik@ifmpan.poznan.pl; Tel: (48-61) 86 12 365; Fax: (48-61) 86 84 524*

[b]*Laboratoire de Chimie du Solide et Moléculaire, UMR 6511, CNRS - Université de Rennes 1, Avenue du Général Leclerc, 35042 Rennes cedex, France*

Received 25th September 2000, Accepted 9th January 2001
First published as an Advance Article on the web 19th February 2001

The isostructural charge-transfer salts κ-$[Et_4N](BEDT\text{-}TTF)_4M(CN)_6\cdot 3H_2O$ ($M = Co^{III}$, Fe^{III}, Cr^{III}) are organic semiconductors undergoing two intriguing phase transitions at $T = 240$ and 150 K. Polarized IR reflectance spectra (from 650 to 6500 cm^{-1}) of these compounds were studied at room temperature. An electronic dispersion in IR spectra was analyzed in terms of a Drude–Lorentz model and optical transport parameters were determined. IR reflectance spectra of Fe^{III} crystals were measured in the temperature range from 190 to 300 K and the influence of the phase transition at 240 K was studied. We report also FT-NIR Raman studies of Fe^{III} salt as a function of temperature from 110 to 300 K. The Raman line related to the $\nu_3(A_g)$ C=C mode of BEDT-TTF splits below 240 K into three components providing evidence of charge redistribution in the BEDT-TTF layers.

1 Introduction

Conducting charge-transfer salts formed by the organic donor bis(ethylenedithio)tetrathiafulvalene (BEDT-TTF) and various acceptors have similar crystal structures consisting of conducting BEDT-TTF layers which alternate with insulating layers of acceptors. A rich variety of electronic states in these salts is mainly due to different types of spatial arrangements of BEDT-TTF molecules inside the layers. The inorganic acceptors compensate the charge and play a crucial role in the interactions between organic layers. Recently, there has been a great interest in the design and study of organic conductors (especially those based on BEDT-TTF or other TTF derivatives) containing anions with permanent magnetic moments.[1–3] It is a striking feature that such compounds combine conducting and magnetic properties and an interesting problem of interactions between itinerant electrons on organic layers with localised spins involved in the counter ions can be studied.

Recently, a series of BEDT-TTF salts with diamagnetic ($M = Co^{III}$, $S = 0$) and paramagnetic ($M = Fe^{III}$, $S = \frac{1}{2}$; $M = Cr^{III}$, $S = \frac{3}{2}$) hexacyanometalate trianions $M(CN)_6^{3-}$ was synthesised. The $M(CN)_6^{3-}$ anions are known to give rise to different kinds of magnetic interactions through the cyano bridges. Depending on the crystal growth conditions, the κ-phase or the β-phase conducting BEDT-TTF layers were obtained.[4,5] The κ-phase crystals of the formula κ-$[Et_4N]$-$(BEDT\text{-}TTF)_4M(CN)_6\cdot 3H_2O$ ($M = Co^{III}$, Fe^{III}, Cr^{III}) are isostructural and exhibit semiconducting properties with the room-temperature electrical conductivities: 10, 0.2 and 0.15 $S\,cm^{-1}$ for Co^{III}, Fe^{III} and Cr^{III} salts, respectively. The crystals undergo two phase transitions at about 240 and 150 K. The consequence of the first transition at 240 K is a structural reorganisation, change of the character of semiconducting behaviour and modification of ESR spectra. On the other hand, the second transition at 150 K was not observed in X-ray crystallographic studies but was evidenced in the heat capacity measurements by an endothermic peak (a characteristic feature of the first-order transitions) and in the thermal dependence of the molar paramagnetic susceptibility. The magnetic data suggest an absence of significant magnetic interactions between the organic and inorganic counterparts.

The crystal structure of the title salts consists of layers of BEDT-TTF donors and $M(CN)_6$ acceptors alternating along the *c*-direction (Fig. 1). At room temperature the organic sublattice is built of two crystallographically independent BEDT-TTF molecules (noted A and B) which are arranged in two different kinds of dimers [Fig. 1(a)]. In all the salts a reversible doubling of the unit cell *a*-parameter is observed at the temperature $T = 240$ K, which remains unchanged down to 115 K at least.[5,6] The crystal structure determined at 215 K revealed that the organic sublattice is built of four crystallographically independent BEDT-TTF molecules (noted A, B, C and D) forming four different kinds of dimers [Fig. 1(b)]. Intramolecular bond lengths of the BEDT-TTF donors from X-ray data were used to estimate the charge distribution inside the conducting layers on the basis of the method proposed in ref. 7. The analysis of X-ray data shows that at room temperature both BEDT-TTF molecules (A and B) bear a charge of +0.5 but below 240 K a redistribution of the charge is observed. At 215 K the charge carried by BEDT-TTF molecules is as follows: 0 on A, +0.5 on B and C, and +1 on D. Charge localisation inside the BEDT-TTF layers was taken into account for interpretation of thermal modifications of the magnetic and electrical properties of the studied materials.[5,6]

Coulomb interactions between electrons play an important role in organic conductors. In the salts based on TTF derivatives the Coulomb interactions are responsible for a competition between the formation of a Mott insulator, due to dimerisation, and the charge ordering of the Wigner crystal type induced by long-range Coulomb interactions. The electronic states of the BEDT-TTF conductors with quarter-filled π-bands (in terms of holes) were studied theoretically by Kino and Fukuyama[8–11] by taking into consideration the anisotropy of transfer integrals between BEDT-TTF molecules and the on-site Coulomb interaction (U) with the Hartee–Fock

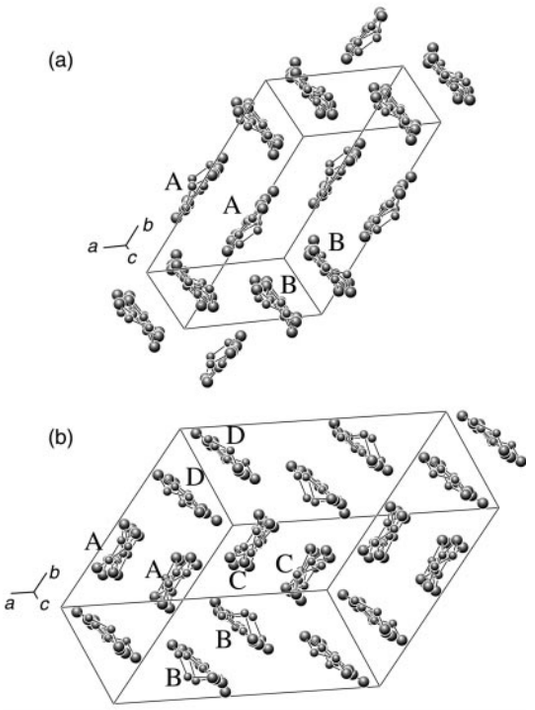

Fig. 1 Structure of conducting BEDT-TTF layers in the crystal κ-$[Et_4N](BEDT\text{-}TTF)_4Fe(CN)_6{\cdot}3H_2O$ at room temperature (a) and at $T=215$ K (b).

approximation. Subsequently, the inter-site Coulomb interactions (V) were also included in the calculations and it was found that these interactions give rise to stripe-type charge ordering states whose charge patterns are strongly dependent on the model parameters.[12,13] In the case of κ-phase BEDT-TTF conductors the insulating state is due to the on-site Coulomb interaction together with strong dimerisation in the conducting layer. In these compounds, spins order ferromagnetically within dimers and the interaction between dimers is antiferromagnetic – these are typical compounds near the Mott transition. It is important to stress that in κ-phase salts the charge distribution is uniform among BEDT-TTF molecules.[8–11]

2 Experimental

The single crystals of κ-$[Et_4N](BEDT\text{-}TTF)_4M(CN)_6{\cdot}3H_2O$ ($M=Co^{III}$, Fe^{III}, Cr^{III}) were obtained on platinum electrodes by electrochemical oxidation of BEDT-TTF solution (solvent: mixture of CH_3CN and CH_2Cl_2) in the presence of the appropriate tetraethylammonium $(Et_4N)^+$ salts of the tri-anions, as described previously.[4] The crystals were in the form of shiny platelets with the best-developed, smooth crystal face (001) being parallel to the conducting BEDT-TTF layers.

Room-temperature polarised reflectance measurements were made on single crystals of all three compounds. The spectra were recorded from the (001) crystal face on a FT-IR Perkin-Elmer 1725X spectrometer in the frequency range from 650 to 6500 cm^{-1}. The spectrometer was equipped with a FT-IR Perkin-Elmer microscope with a liquid-nitrogen-cooled MCT bolometer as the detector. The IR beam was polarised with a gold-wire grid on an AgBr substrate. For low temperature measurements the samples were mounted in a nitrogen-cryostat (THMS 600 Linkam freezing–heating stage), regulated by a temperature controller. The polarised reflectance was studied for the Fe^{III} salt in the temperature range 190–300 K, concentrating on the phase transition temperature $T=240$ K. The thermal dependence of the spectra was studied for samples cooled down with a temperature variation rate of 1 K min^{-1}.

The frequency dependent optical conductivity was obtained by Kramers–Kronig analysis of the reflectance data. The low-frequency data were extrapolated to zero-frequency assuming a constant value, a common procedure for semiconducting materials. The high-frequency data were extended on the basis of the reflectance spectra of the salt κ-$(BEDT\text{-}TTF)_2Cu(NCS)_2$ in the frequency region 6500–30 000 cm^{-1} [14] and above 30 000 cm^{-1} as $R\approx\omega^{-2}$. Despite the reflectance being measured in a relatively narrow frequency range, we believe that a Kramers–Kronig analysis with such an extrapolation procedure yields good infrared conductivity spectra, since IR reflectance spectra of all the κ-phase BEDT-TTF salts are very similar to each other.[14–16]

Raman data for the Fe^{III} salt were obtained using a Bruker Fourier IFS 66 spectrometer with a FRA 106 Raman attachment, which operates with a Nd:YAG laser with a wavelength of 1064 nm. In the case of organic conductors the strong electronic absorption yields the problem of sample overheating. To reduce the heating problem the crystals were ground to powder with KBr and then slightly pressed into a small hole in an aluminium plate. This enabled us to increase the laser power and Raman signal without the risk of sample decomposition. The laser beam was defocused and its power kept below 30 mW. Raman spectra were accumulated during 100 min (3000 accumulations) and the resolution was set at 4 cm^{-1} in order to obtain an acceptable signal-to-noise ratio. Low temperature measurements were performed with the sample mounted in a continuous-flow liquid-nitrogen Linkam THMS 600 cryostat operating within the temperature range 100–300 K. Similarly as in IR experiments, the temperature was decreased very slowly with the rate of 1 K min^{-1} and carefully stabilised.

3 Results

3.1 Infrared studies

Fig. 2 shows the room-temperature reflectance spectra of κ-$[Et_4N](BEDT\text{-}TTF)_4M(CN)_6{\cdot}3H_2O$ ($M=Co^{III}$, Fe^{III}, Cr^{III})

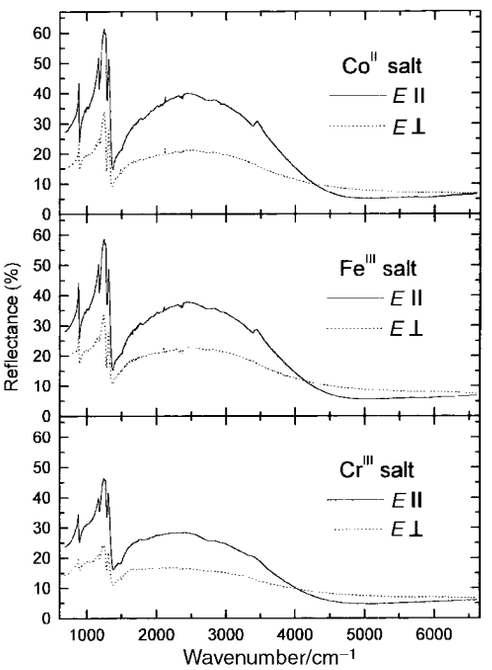

Fig. 2 Polarised reflectance spectra of κ-$[Et_4N](BEDT\text{-}TTF)_4M(CN)_6{\cdot}3H_2O$ ($M=Co^{III}$, Fe^{III}, Cr^{III}) single crystals at room temperature for two perpendicular polarisations of the IR beam.

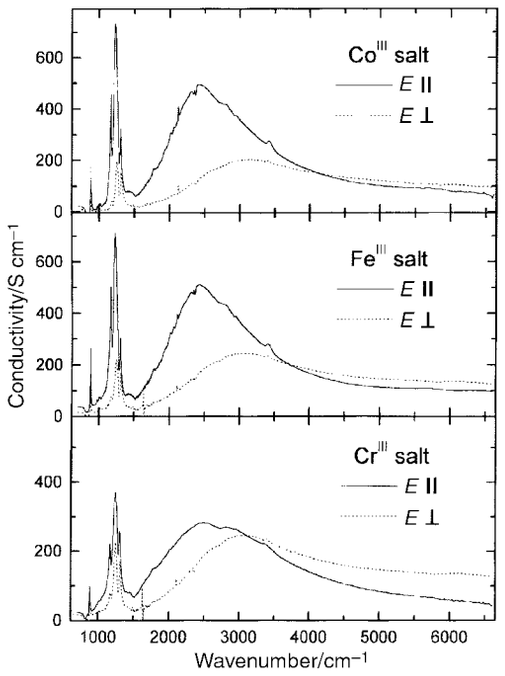

Fig. 3 Infrared conductivity spectra of κ-[Et_4N](BEDT-TTF)$_4$M(CN)$_6$·3H_2O (M = Co^{III}, Fe^{III}, Cr^{III}) crystals at room temperature as obtained from the reflectance spectra by the Kramers–Kronig transformation.

single crystals from the (001) crystal face, for two perpendicular orientations of the electrical vector of the polarised light, corresponding to the maximum ($E\|$) and minimum ($E\perp$) of reflected energy, respectively. For polarisation $E\|$, the electrical vector was parallel to the direction [110], *i.e.* the direction of the strongest side-by-side S···S contacts between neighbouring BEDT-TTF molecules. Each spectrum consists of a strong, broad electronic absorption with a maximum at *ca.* 2500 cm^{-1}, corresponding to the charge transfer between BEDT-TTF moieties, and vibrational structure below 1400 cm^{-1} due to the A_g vibrations of BEDT-TTF (mainly C=C stretching), activated by coupling with the electronic excitation. Additionally, some weaker bands related to the IR active vibrations of BEDT-TTF are observed. The band at 880 cm^{-1} is attributed to the activated mode $\nu_{60}(B_{3g})$ of BEDT-TTF according to the assignment proposed in ref. 17. The spectra of all the salts are very similar to each other and are typical for κ-phase BEDT-TTF salts.[14–16] Similarity of the spectra for two perpendicular polarisations indicates that the compounds exhibit small electronic anisotropy within the conducting BEDT-TTF layers.

The optical conductivity spectra derived by the Kramers–Kronig transformation are displayed in Fig. 3. The spectra show conductivity maxima at *ca.* 2400 cm^{-1} for $E\|$ and *ca.* 3100 cm^{-1} for $E\perp$. Such behaviour suggests the presence of an optical energy gap, in agreement with the electrical conductivity data.[4] In order to analyse this electronic dispersion we made least-squares fits to the experimental data of the reflectance calculated from a Drude–Lorentz dielectric function of the

Table 1 Parameters of the Drude–Lorentz fits to the reflectance spectra of κ-[Et_4N](BEDT-TTF)$_4$M(CN)$_6$·3H_2O (M = Co^{III}, Fe^{III}, Cr^{III}) salts for polarisation $E\|$ and $E\perp$

	Co^{III}		Fe^{III}		Cr^{III}	
Salt	$E\|$	$E\perp$	$E\|$	$E\perp$	$E\|$	$E\perp$
ε_∞	4.0	3.8	4.1	4.1	3.5	3.5
ω_p/cm^{-1}	6800	5300	6700	5700	5800	4900
Γ/cm^{-1}	1700	2600	1700	2700	2100	3300
ω_0/cm^{-1}	2500	3300	2600	3200	2700	3300

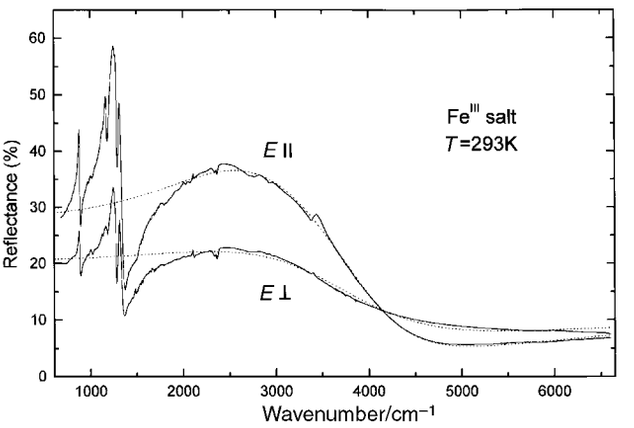

Fig. 4 Room-temperature reflectance spectra of Fe^{III} salt with the Drude–Lorentz fits (dotted lines).

form

$$\varepsilon(\omega) = \varepsilon_\infty + \frac{\omega_p^2}{\omega_0^2 - \omega^2 - i\omega\Gamma} \quad (1)$$

where ω_0 is the centre frequency (energy gap), ω_p is the plasma frequency, Γ is the relaxation rate and ε_∞ represents all higher frequency contributions to the dielectric function. The fits were made to the reflectance between 1900 and 6500 cm^{-1}. Below 1900 cm^{-1} both electron–phonon and electron–electron interactions yield distinct deviations from the simple Drude–Lorentz behaviour, as seen in Fig. 2. The best results are listed in Table 1 and an exemplary fit is shown (Fig. 4) for the Fe^{III} spectrum (analogous fit qualities were obtained for other salts).

To compare the spectral differences between the phases above and below the phase transition at $T = 240$ K, we show the reflectance spectra and frequency-dependent conductivity of the Fe^{III} crystals for three temperatures in Fig. 5 and Fig. 6. As the temperature decreases the oscillator strength of the charge-transfer band gradually grows and then below 240 K decreases. To analyse thermal evolution of the electronic band in more detail we have fitted the reflectance data by the

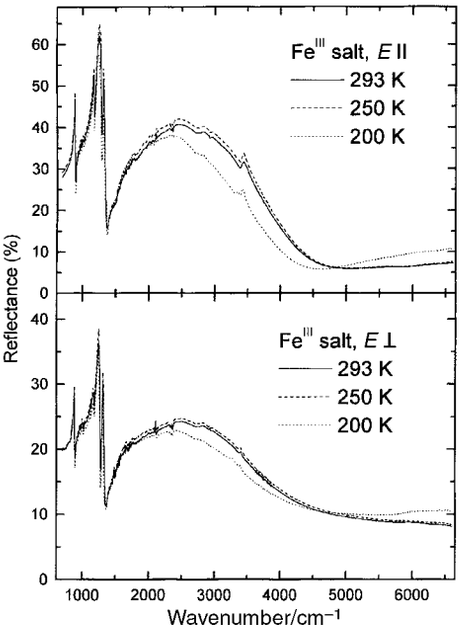

Fig. 5 Temperature dependence of the polarised reflectance spectra obtained from the (001) crystal face of the Fe^{III} salt for two perpendicular polarisations.

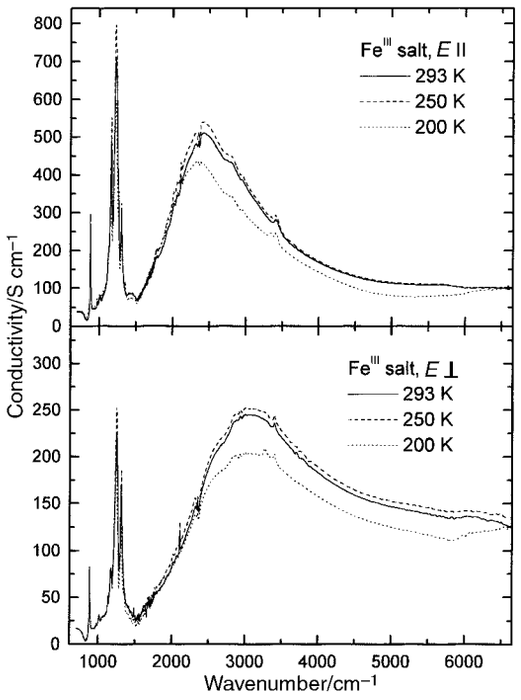

Fig. 6 Temperature dependence of the conductivity spectra of the Fe^{III} salt for two perpendicular polarisations.

function (1). The optical transport parameters determined from this analysis are displayed in Fig. 7. The parameters of the Drude–Lorentz model undergo considerable modifications for both polarisations: the energy gap (ω_0) decreases by *ca.* 200 cm^{-1} for $E\|$ and 100 cm^{-1} for $E\perp$, with an abrupt change at 240 K; the plasma frequency (ω_p) changes its character of the thermal dependence at 240 K and then below this temperature decreases; the relaxation rate (Γ) also undergoes considerable modifications.

3.2 Raman studies

Fig. 8 shows the FT-NIR Raman spectra of κ-[Et_4N](BEDT-TTF)$_4$Fe(CN)$_6$·3H_2O from 100 to *ca.* 2000 cm^{-1} at three different temperatures. The assignment of Raman active, mainly the totally symmetric A_g modes, was made on the basis of data for the neutral BEDT-TTF molecule,[18] its cation-radical[19] as well as the Raman spectra of other κ-phase salts of BEDT-TTF.[16,17,20,21] At room temperature the A_g modes of BEDT-TTF are observed at the following frequencies: $\nu_2=1498$, $\nu_3=1459$, $\nu_4=1422$, $\nu_5=1278$, $\nu_6=988$, $\nu_9=499$, $\nu_{10}=451$, $\nu_{11}=320$, and $\nu_{12}=165$ cm^{-1} [the $\nu_1(A_g)$ and $\nu_8(A_g)$ modes were not detected even at low temperature]. The strong band at 893 cm^{-1} should be related to the non-totally symmetric mode $\nu_{60}(B_{3g})$, according to the assignment proposed in refs. 17 and 21. At room temperature the spectral feature at 893 cm^{-1} consists of two lines since at lower temperatures, when the peaks get sharper, the $\nu_7(A_g)$ mode at 898 cm^{-1} can also be distinguished. On the other hand, the broad structure in the region 980–1050 cm^{-1} is due to the superposition of the modes $\nu_6(A_g)=988$ cm^{-1} as well as $\nu_{58}(B_{3g})=1005$ cm^{-1}. Within the region 1300–1600 cm^{-1} (C=C vibrations) the room-temperature spectrum is dominated by the band at $\nu_3(A_g)=1459$ cm^{-1}, while the bands for $\nu_2(A_g)=1498$ cm^{-1} and $\nu_4(A_g)=1422$ cm^{-1} are only seen as weak spectral features superimposed on the wings of the $\nu_3(A_g)$ peak. These frequencies correspond quite well to the frequencies of BEDT-TTF molecules with formal charge +0.5 observed in other κ-phase salts.[16,17,20,21]

On lowering the temperature the intensity of all Raman bands grows considerably but the strongest intensity enhancement is observed for the band at 1413 cm^{-1} below 240 K (Fig. 9). We suggest that this enhancement is due to a gradual increase of the concentration of BEDT-TTF molecules with the charge +1. At low temperature this band is a superposition of the weak component $\nu_4(A_g)=1422$ cm^{-1} of BEDT-TTF$^{0.5+}$ and the overwhelming contribution of $\nu_3(A_g)=1413$ cm^{-1} of the BEDT-TTF$^+$ ion. In ref. 19 the $\nu_3(A_g)$ mode of the BEDT-TTF$^+$ radical cation is observed at 1431 cm^{-1}, *i.e.* in the case of the Fe^{III} salt this vibration has a lower frequency. Simultaneously, with an increase in the concentration of

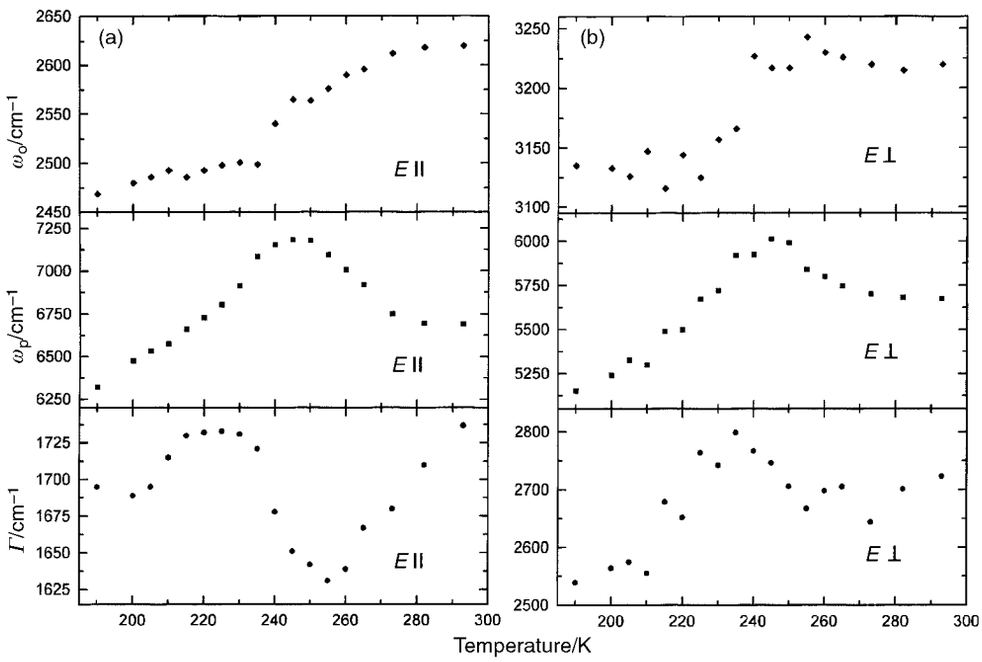

Fig. 7 Temperature dependence of the energy gap (ω_0), plasma frequency (ω_p) and scattering rate (Γ) for the Fe^{III} salt as obtained by the Drude–Lorentz fits to the reflectance data for polarisation $E\|$ (a) and $E\perp$ (b).

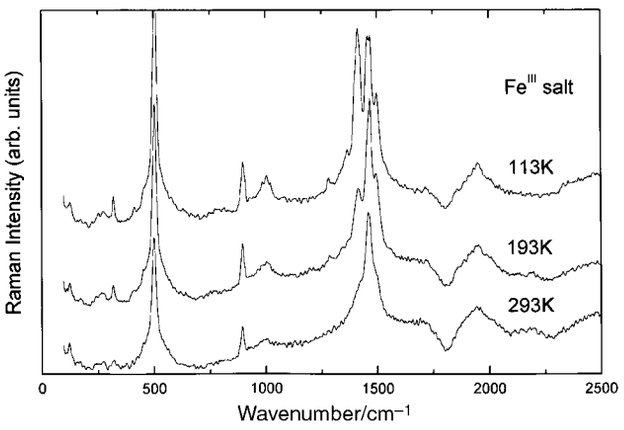

Fig. 8 FT-NIR Raman spectra of powdered Fe^{III} crystals at three different temperatures (excitation wavelength 1064 nm).

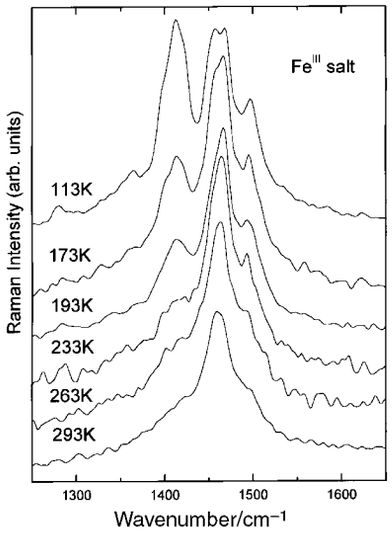

Fig. 9 Temperature dependence of the FT-NIR Raman spectra of the Fe^{III} salt within the region of C=C vibrations of BEDT-TTF.

$BEDT\text{-}TTF^{+}$ ions, the concentrations of $BEDT\text{-}TTF^{0.5+}$ and $BEDT\text{-}TTF^{0}$ molecules should decrease and increase, respectively. This is partially observed in our Raman spectra: the band at $1459\ cm^{-1}$ decreases in intensity but the band at $1498\ cm^{-1}$ does not become evidently stronger (Fig. 9). Analogously to the above interpretation of the $1413\ cm^{-1}$ peak we propose that at low temperatures the component at $1498\ cm^{-1}$ is to be assigned to a superposition of the weak

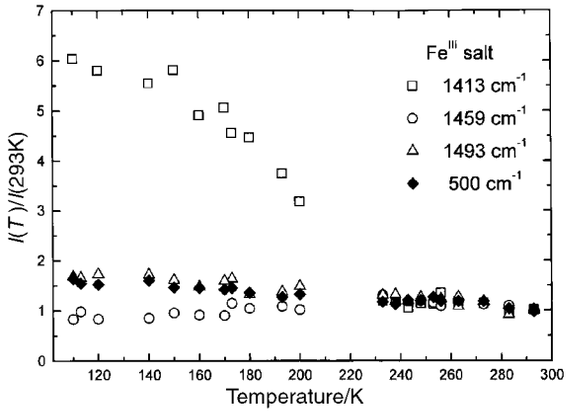

Fig. 10 Temperature dependence of the integral intensities of selected FT-NIR Raman bands of the Fe^{III} salt.

$\nu_2(A_g)$ band of $BEDT\text{-}TTF^{0.5+}$ and the strong $\nu_3(A_g)$ band of $BEDT\text{-}TTF^{0}$ ($1493\ cm^{-1}$ in ref. 18).

To analyse the thermal evolution of C=C Raman bands, the vibrational features from 1300 to $1600\ cm^{-1}$ were deconvoluted into separate components. The temperature dependence of the integral intensities of the bands related to the $\nu_3(A_g)$ mode of BEDT-TTF bearing the charge 0, +0.5, +1 is shown in Fig. 10. A striking feature is that charge disproportionation does not occur abruptly at the phase transition temperature of 240 K but it is gradually developed below 240 K. In Fig. 10 we show also for comparison the temperature dependence of the intensity of the $\nu_9(A_g) = 500\ cm^{-1}$ band. It should be noted that, although the frequency of the $\nu_9(A_g)$ mode depends upon the charge residing on the BEDT-TTF molecule,[19] the appropriate Raman feature seems to be a single line even at lowest temperatures.

4 Discussion

As expected for isostructural compounds, the reflectance spectra are qualitatively very similar; nevertheless, some quantitative differences can be found (Fig. 2 and Fig. 3). The spectra of the Co^{III} and Fe^{III} salts are nearly the same but the absolute values of reflectance for the Cr^{III} salt (and hence optical conductivity values) are lower. These differences are well described by the optical transport parameters determined from Drude–Lorentz fits. As the results from Table 1 show, these parameters for Co^{III} and Fe^{III} salts are nearly the same, whereas for Cr^{III} for both polarisations the respective plasma frequencies are smaller, the energy gaps and the relaxation rates are larger. This can be related to small differences between the crystallographic parameters. All the compounds crystallise in the triclinic unit cell and are isostructural; nevertheless, there are slight differences between the unit cell parameters.[6] For example, the *a*-parameter is 8.945, 8.949 and 8.967 Å for Co^{III}, Fe^{III} and Cr^{III} salts, respectively. Considering the unit cell volume one can conclude that the BEDT-TTF molecules in the Cr^{III} salt crystallise slightly more 'loosely' in comparison to Co^{III} and Fe^{III}, and this may be the reason for the observed spectral differences.

Important changes in the electronic spectrum of the Fe^{III} salt occur as a result of the phase transition at 240 K (Fig. 5 and 6). In the phase above 240 K, the oscillator strength of this band increases systematically in both polarisations with decreasing the temperature. Consequently, the plasma frequency grows but the energy gap and the relaxation rate decrease. Such behaviour of transport parameters can be related to an increase of transfer integrals, as a result of the contraction of the unit cell volume on lowering the temperature. In the phase below 240 K, the oscillator strength of electronic band decreases and, simultaneously, reflectance in the high-frequency part of the spectra grows. Such behaviour is a consequence of the charge redistribution, which develops below 240 K. The electronic band at *ca.* $3000\ cm^{-1}$, related to charge transfer between charged and neutral molecules, decreases since the number of $BEDT\text{-}TTF^{0.5+}$ cations decreases. Simultaneously, the band related to charge transfer between two charged molecules should grow since there are more $BEDT\text{-}TTF^{+}$ cations. This band is observed in the BEDT-TTF salt at *ca.* $10\,000\ cm^{-1}$, *i.e.* in the region not measured in our experiment; nevertheless, above $5000\ cm^{-1}$ we see a wing of this absorption and its intensity increases, in agreement with our expectations.

The Raman data provide an unambiguous proof of the gradual charge redistribution below 240 K. As mentioned in the introduction, charge ordering phenomena are rather common in quarter-filled quasi-two-dimensional BEDT-TTF salts but, to our knowledge, they have not been observed in κ-phase crystals as yet. Recently, it was found that the intersite Coulomb interactions (V) give rise to stripe-type charge

ordering states in BEDT-TTF salts, whose charge patterns are dependent on the parameters of the model.[12] The charge ordering states due to intersite Coulomb interaction can be widely realised in two-dimensional salts with insulating behaviour on the condition that they are not dimerised, *i.e.* they are not κ-type compounds. The presence of the relevant values of V can be also expected in κ-phase salts; however, the stability of the dimeric antiferromagnetic state in their insulating phase is proved by the mean-field calculations considering only the on-site Coulomb repulsion U (without V). Obviously, the stability of this state is also confirmed by existing experimental data. It is surprising that, though the studied crystals are κ-type, they are not stable and show charge ordering. The reason for such behaviour could be the weakness of interactions of BEDT-TTF molecules forming the dimer in comparison to interdimer interactions. At room temperature the intradimer distances between the planes of BEDT-TTF are equal to 3.63 and 3.80 Å for A and B dimers, respectively, whereas in the majority of κ-type salts this parameter is smaller (*ca.* 3.35 Å).[6] In our compounds the dimerisation is not very strong, therefore, they may be considered quarter-filled κ-type compounds (not half-filled). The κ-phase BEDT-TTF salts are stable when the dimerisation in BEDT-TTF layers is strong, since the electron correlation results in a Mott insulating state due to a half-filled band. On the other hand, it can be suggested that a unique feature of these crystals is that the intersite Coulomb repulsions (V) cannot be neglected, and below 240 K they yield charge ordering phenomena, so unexpected in κ-phase crystals.

The charge redistribution is not an abrupt process but develops gradually below 240 K, *i.e.* the concentration of BEDT-TTF^{+} and BEDT-TTF^{0} molecules increases gradually and, obviously, their position within the crystal lattice is not fixed but changes dynamically. When the concentration is high enough, the formation of a charge-ordered superstructure can be expected. Such phenomena were observed in charge-transfer salts formed by the donor TMTSF (tetramethyltetraselenafulvalene) with various counter-anions. In these compounds the structure does not exhibit any changes through a transition into a charge localisation state (a so-called structureless transition).[22,23] A similar transition can be expected in our crystals at 150 K. Preliminary IR studies of the Co^{III} salt show that at 150 K a new energy gap in the electronic excitation spectrum is formed,[24] though the X-ray studies did not reveal any structural variation. Therefore, one can suggest that at 150 K a new charge-ordered state is formed due to long-range electron–electron correlation.

Acknowledgements

This work was supported by KBN under grant 2 P03B 112 12.

References

1 L. Ouahab, *Chem. Mater.*, 1997, **9**, 1909.
2 P. Day and M. Kurmoo, *J. Mater. Chem.*, 1997, **7**, 1291.
3 E. Coronado, J. R. Galán-Mascarós and C. J. Gómez-García, *J. Chem. Soc., Dalton Trans.*, 2000, 205.
4 P. Le Maguerès, L. Ouahab, N. Conan, C. J. Gómez-García, P. Delhaès, J. Even and M. Bertault, *Solid State Commun.*, 1996, **97**, 27.
5 P. Le Maguerès, L. Ouahab, P. Briad, J. Even, M. Bertault, L. Toupet, J. Rámos, C. J. Gómez-García, P. Delhaès and T. Mallah, *Synth. Met.*, 1997, **86**, 1859.
6 P. Le Maguerès, Ph.D. Thesis, Université de Rennes, 1995, pp. 123–140.
7 P. Guionneau, C. J. Kepert, D. Chasseau, M. R. Truter and P. Day, *Synth. Met.*, 1997, **86**, 1973.
8 H. Kino and H. Fukuyama, *J. Phys. Soc. Jpn.*, 1995, **64**, 1877.
9 H. Kino and H. Fukuyama, *J. Phys. Soc. Jpn.*, 1995, **64**, 2726.
10 H. Kino and H. Fukuyama, *J. Phys. Soc. Jpn.*, 1995, **64**, 4523.
11 H. Kino and H. Fukuyama, *J. Phys. Soc. Jpn.*, 1996, **65**, 2158.
12 H. Seo, *J. Phys. Soc. Jpn.*, 2000, **69**, 805.
13 H. Fukuyama and H. Seo, *J. Phys. Soc. Jpn. Suppl.*, 2000, **69**, 144.
14 T. Sugano, H. Hayashi, M. Kinoshita and K. Nishikida, *Phys. Rev. B*, 1989, **39**, 11 387.
15 R. Masuda, H. Tajima, H. Kuroda, H. Mori, S. Tanaka, T. Mori and H. Inokuchi, *Synth. Met.*, 1993, **55–57**, 2489.
16 J. E. Eldridge, Y. Xie, Y. Lin, C. C. Homes, H. H. Wang, J. M. Williams, A. M. Kini and J. M. Schlueter, *Spectrochim. Acta Part A*, 1997, **53**, 565.
17 J. E. Eldridge, Y. Xie, H. H. Wang, J. M. Williams, A. M. Kini and J. M. Schlueter, *Spectrochim. Acta Part A*, 1996, **52**, 45.
18 J. E. Eldridge, C. C. Homes, J. M. Williams, A. M. Kini and H. H. Wang, *Spectrochim. Acta Part A*, 1995, **51**, 947.
19 M. E. Kozlov, K. I. Pokhodnia and A. A. Yurchenko, *Spectrochim. Acta Part A*, 1989, **45**, 437.
20 S. Sugai, H. Mori, H. Yamochi and G. Saito, *Phys. Rev. B*, 1993, **47**, 14 374.
21 J. E. Eldridge, Y. Lin, H. H. Wang, J. M. Williams and A. M. Kini, *Phys. Rev. B*, 1998, **57**, 597.
22 J. P. Pouget and S. Ravy, *J. Phys. I (France)*, 1996, **6**, 1501.
23 J. P. Pouget and S. Ravy, *Synth. Met.*, 1997, **85**, 1523.
24 R. Świetlik, *et al.* – to be published.